COMPARATVE STUDY OF RADIATION CHARACTERISTICS OF VARIOUS MICROSTRIP MIC ELEMENTS

Nagayoshi MORITA and Katsuhito OHNO
Chiba Institute of Technology
2-17-1, Tsudanuma, Narashino-shi, Chiba, 275-0016, Japan
E-mail: moritan@ec.it-chiba.ac.jp

1. Introduction

Monolithic-type microwave integrated circuits used in various communication devices have many microstrip discontinuities such as ends, bends, gaps, and width changes. Such circuits are usually designed assuming no radiation from these discontinuities. However, radiation always occurs more or less because the structure is theoretically of open type. Recent trend of use of higher frequency and densely compacted circuits necessitates careful consideration of influence of such radiation on circuit characteristics and surrounding environment. Nevertheless, little work has been done on how radiation characteristics differ by the difference of discontinuities, or by frequency change[1]. The reason is that no pertinent means have been available to evaluate accurately radiation properties, both radiation patterns and radiated powers. The authors have developed a new method combining FD-TD method and radiation mode theory, which makes it possible to calculate radiation patterns and radiated powers in both space region and substrate region [2],[3]. In the present paper, by using this new method, radiation properties are analyzed very accurately, and comparative studies of radiation characteristics are undertaken by taking several typical microstrip-type circuit elements as examples. Summarized results are presented by putting these elements together into four groups, each group including elements with similar shape and similar radiation characteristics: bends and mitered bends are put in group 1, ends, gaps, and steps are collected in group 2, stubs are put in group3, and double-beam couplers and parallel line couplers are in group 4.

2. Common features to all examples

All numerical examples are given for the element structures of which straight line parts are consisted of $50\,\Omega$ microstrip lines with substrate thickness h being 0.6mm, relative permittivity ε_r being 10.0, frequency f being 10GHz, and strip width w being 0.6mm, if nothing specified. Conductor and dielectric losses are not considered.

Relative error of numerical computation E_r is evaluated using the energy conservation relation:

$$E_r = \left| \left(P_{tra} + P_{ref} + P_{sub} + P_{spa} \right) - P_{inc} \right| / P_{inc} \qquad (1)$$

where P_{inc} is the incident guided mode power, P_{tra} and P_{ref} are, respectively, transmitted and reflected guided mode power, which correspond to S_{21} and S_{11}, respectively, while P_{sub} is the radiated power scattered into the substrate region as surface wave mode and P_{spa} is the radiated power scattered into the space (air) region. All these powers are calculated based on reaction integrals between fields on certain surface obtained by the FD-TD method and the corresponding mode (guided or radiation mode) fields on the same surface. These modes become guided modes for calculation of P_{tra} and P_{ref}, and radiation modes for calculation of P_{sub} and P_{spa} [2],[3].

Absorbing boundary used in the FD-TD calculation is PML(Perfectly Matched Layer) with 10 layers. In most cases non-equal mesh divisions are used with maximum to minimum ratio being around 2.0. Edges of strip conductors are not coincident with mesh coordinates but are taken length 0.0 to 0.5δ shifted from mesh lines where δ is a mesh size. Higher accuracy is aimed at by employing this meshing scheme where the integral form of Maxwell's equations is utilized to calculate magnetic fields at the points nearest to strip edges.

3. Group 1 – Right-angled bends

Figure 1 shows mitered right-angled bends together with the Cartesian coordinates used here. Size of cut part from the corner point is assumed to be the same as the strip width for simplicity. S parameters and radiated powers are shown in Table 1 and radiation patterns in the XY and XZ, and YZ planes are given in Fig.2. Radiated powers in Table 1 are normalized by the incident power, which

ISBN: 4-88552-206-4 C3055©IEICE

holds also for the cases of other elements presented hereafter. Radiation patterns in Fig.2 are all described with maximum being 0dB and minimum being –50dB, which applies also to all radiation patterns shown hereafter. Comparing mitered bends with simple (un-mitered) bends, transmitted power is seen to be made small as expected, but the amount of radiated power, both into space and into substrate, is seen to be almost the same. As for the radiation patterns in the space region, i.e. those in the XZ and YZ planes, all patterns have similar semicircular shape, since the discontinuity sizes causing radiation are very small compared to the wavelength. However, we observe by a careful inspection that more power is pulled toward the direction to which strip lines extend than other directions. As regards the radiation into the substrate region, i.e. that in the XY plane, more power is radiated in the directions of $45°$ and $240°$ than other directions for both mitered and simple bends.

4. Group 2 − Ends, gaps, and steps

Figure 3 (a), (b), and (c) illustrate the strip conductor shapes treated in this group. S parameters and radiated patterns are listed in Table 2, and radiation patterns are described in Fig.4 (a), (b), and (c). Values in Table 2 represent typical features for each element; for example, reflected power and radiated power are by far smaller in steps than in ends and gaps. The beam width of lobe in radiation patterns is narrower in the XZ plane than in the YZ plane for all three elements. We notice that the pattern in the XY plane for the step is asymmetric with respect to the x axis. This is because the upper step width is a little smaller than the lower one as shown in Fig.3 (c).

5. Group 3 − Stubs

Typical three types of stub shapes as illustrated in Fig.5, i.e., open, radial, and gamma-shaped stubs, are examined here. For open stubs and radial stubs, frequency dependence of radiated powers is shown in Fig.6, from which it is observed that radiated powers both into space region and substrate region increase up to around 10GHz and then only the space region radiated power decreases gradually with frequency. Thus, further increase in frequency will yield surpass of substrate region radiated power over space region radiated power, which fact is already indicated in Ref.[1]. This property seems to apply also to other similar element structures such as bends, ends, and gaps, although details are not investigated yet. In the case of radial stubs, however, both space and substrate region radiated powers seem to increase as frequency goes up as seen from Fig.6 (b). Reflected power becomes very large at around 8.5GHz and 7GHz for open stubs and radial stubs, respectively, with the dimensions chosen here. Radiation patterns for these cases of large reflection (small transmission) assume like Fig.7. To compare with these, radiation patterns for the case of very small reflection (large transmission) are depicted in Fig.8, where 14GHz is set for this purpose. Patterns in the XZ and YZ planes are omitted since those are not much different from those of Figs.7 (b) and (c). As regards radiation patterns for the case where reflected power dominates, we see from Fig.7 (a) that radiated power in the substrate region propagates in the direction orthogonal to the original straight line, that is, $90°$ and $270°$ in the case of open stub, whereas in the case of radial stub the radiation directions are slightly inclined from orthogonal directions to $60°$ and $240°$. As regards radiation patterns when transmitted power dominates, Fig.8 shows us that maximum radiation is directed toward $80°$ and $260°$ in the case of radial stub, although that for open stub is the same as in the case of large reflection, i.e., $90°$ and $270°$. Thus, it seems that the radiation direction does not change with frequency in the case of open stub but moves slightly with frequency in the case of radial stub. Also noticed is that the radiated power in the direction of $180°$ is very small in both open stub and radial stub because the example of Fig.8 is for the case of small reflection. The lobe width in the space region radiation pattern is narrower in the XZ plane than that in the YZ plane. Radiated power from a gamma-shaped stub st 10GHz are listed in Table 3. At this frequency, transmitted power dominates , for which radiation patter in the XY plane is calculated and superposed in Fig.8. Those in the XZ and YZ planes are omitted because they are similar to those of Figs.7 (b) and (c). As seen from Fig.8, surface wave looks to propagate relatively strongly in particular directions in the case of gamma stub, $70°$ and $240°$ in this example. We must recognize, from Figs. 7 and 8, rather general interesting features such that stronger radiation in the substrate region occurs not only in the direction of stubs extending but also in their opposite directions. Relative error E_r evaluated by means of eq.(1) is less than 1.0% for all numerical examples shown thus far in this paper.

6. Group 4 − Couplers

Two types of couplers are examined here; one is double beam coupler and the other is parallel

line coupler as shown in Fig.9. In the former type couplers, h and ε_r are the same as those of the examples treated in the preceding sections, while in the latter type couplers, h is the same as that used thus far but ε_r is chosen to be 15.7 for realizing suitable coupling behavior. Furthermore, dimensions with respect to the structure of Fig.9 (a) and (b) are set to have maximum power transmission at around 10GHz and 12GHz, respectively. Figures 10 shows frequency characteristics of radiated powers for the two types of couplers, which shows that radiated powers are relatively small at around this frequency range although they tend to increase as frequency goes up. Radiation patterns of double beam coupler at 10.5GHz and parallel line coupler at 11.5GHz in the XY plane are depicted in Fig.11, from which we observe that the direction of surface wave advancing is similar to the elements of group 2 although the maximum directions are inclined about $10°$ in the double beam coupler. Radiation patterns in the XZ and YZ planes are similar to those of group 2 and omitted here. Relative error E_r is about 1.0% or less for the examples in this section.

7. Conclusions

Radiation characteristics are investigated for ten typical microstrip MIC passive elements. Comparative studies are carried out, for the first time, on the basis of accurate numerical analysis to clear similarities and differences of radiation characteristics when element shapes and frequency differ. Radiation patterns in the space region are generally of the shape of semicircle although some differences can be noticed such that the lobe beam width is narrower in the plane perpendicular to the strip line extending than in the plane parallel to it when elements are of ends, gaps, steps, and couplers and the property is opposite for other elements such as various types of stubs. On the other hand, the maximum radiation directions change variously in the substrate region. It is a distinctive feature on the surface wave radiation that stronger radiation occurs not only in the direction of the strip line extending but also in their opposite directions. Comparative studies for other types of various elements not taken up in this paper as well as those for slot line discontinuities and cpw discontinuities remain as future important subjects.

References

[1]T.S.Horng, S.C.Wu, H.Y.Yang, and N.G.Alexopoulos,"A generalized method for distinguishing between radiation and surface-wave losses in microstrip discontinuities," IEEE Trans. Microwave Theory Tech., Vol.38, No.12, pp.1800-1807, Dec. 1990.

[2]N.Morita, "A new formulation for radiated fields using radiation mode expansions and its application to radiation from microstrip antennas," Trans.IEICE, Japan, E77-C, No.11, pp.1795-1801, Nov. 1994.

[3] N. Morita, Y. Yoshioka, and N. Hosoya, "Development of an analysis method and its simulation tool for microstrip-type microwave integrated circuit elements," Trans.IEICE, Japan, E84-C, No.7, pp.898-904, July, 2001.

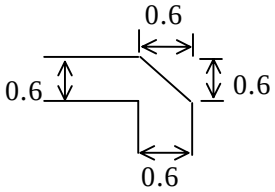

Fig.1. Mitered right-angled bend (in mm).

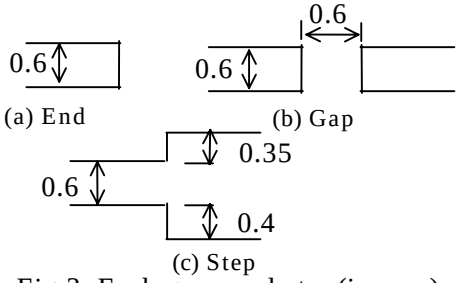

Fig.3. End, gap, and step(in mm).

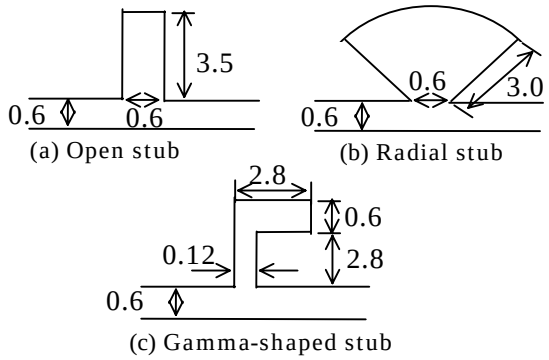

Fig.5. Stubs(in mm).

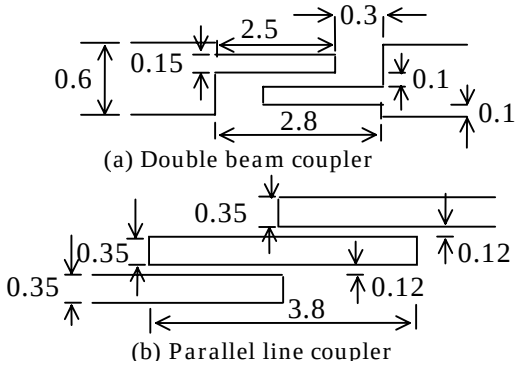

Fig.10. Couplers(in mm).

Table 1 Radiated powers of bends.

	Simple	Mitered
S_{11}(dB)	-13.2269	-16.9726
S_{21}(dB)	-0.2101	-0.0847
P_{spa}	0.0052	0.0051
P_{sub}	0.0017	0.0017

Table 2 Radiated powers of end, gap, and step.

	end	gap	step
S_{11}(dB)	-0.0194	-0.0270	-6.5651
S_{21}(dB)	------	-12.6035	-0.1229
P_{spa}	0.0067	0.0071	0.0003
P_{sub}	0.0021	0.0023	7.9144×10^{-5}

Table 3 Radiated powers of gamma stub.

S_{11}(dB)	-13.6321
S_{21}(dB)	-0.01479
P_{spa}	0.0067
P_{sub}	0.0012

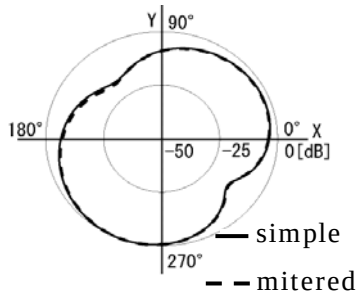

(a) XY plane

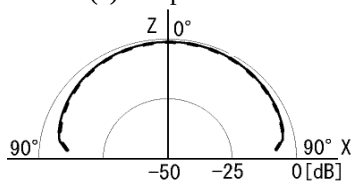

(b) XZ plane

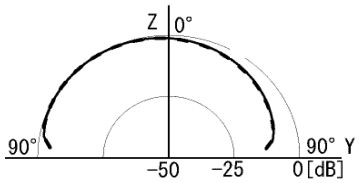

(c) YZ plane

Fig.2. Radiation patterns of simple and mitered bends.

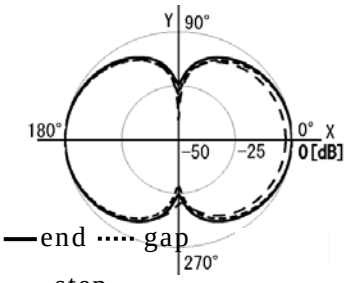

(a) XY plane

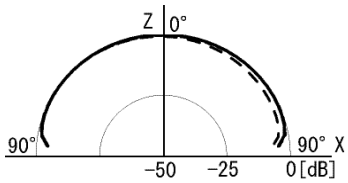

(b) XZ plane

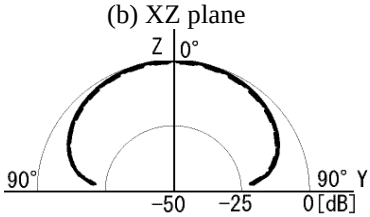

(c) YZ plane

Fig.4. Radiation patterns of end, gap, and step.

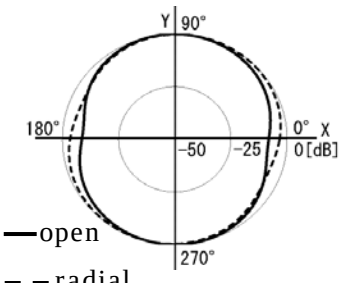

(a) XY plane

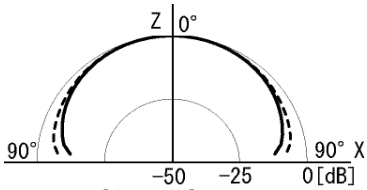

(b) XZ plane

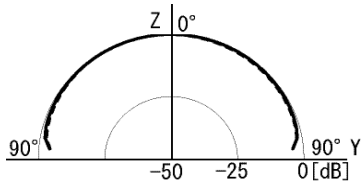

(c) YZ plane

Fig.7. Radiation patterns of open and radial stubs for large reflection.

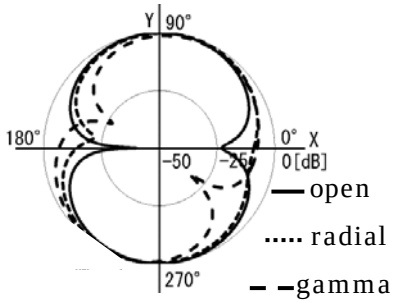

Fig.8. Radiation patterns of stubs in the XY plane for large transmission.

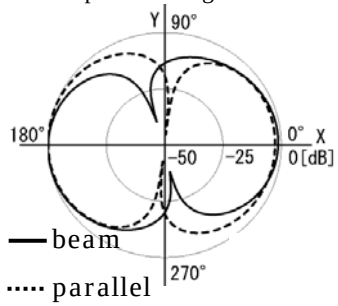

Fig.11. Radiation patterns of couplers in the XY plane

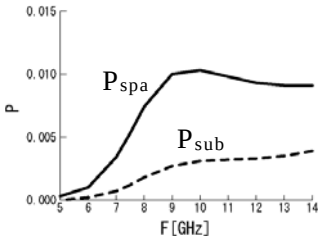

(a) Open stub

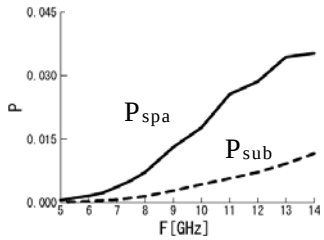

(b) Radial stub

Fig.6. Radiated powers from open and radial stubs.

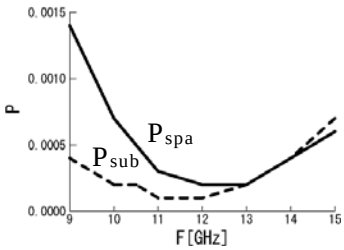

(a) Double beam coupler

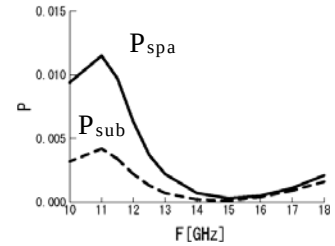

(b) Parallel line coupler

Fig.10. Radiated powers from two types of couplers.